



Accurate Lithium-ion battery parameter estimation with continuous-time system identification methods



Bing Xia^{a,b}, Xin Zhao^c, Raymond de Callafon^c, Hugues Garnier^{d,e}, Truong Nguyen^b, Chris Mi^{a,*}

^a Department of Electrical and Computer Engineering, San Diego State University, 5500 Campanile Drive, San Diego, CA 92182, USA

^b Department of Electrical and Computer Engineering, University of California San Diego, 9500 Gilman Dr., La Jolla, CA 92093, USA

^c Department of Mechanical and Aerospace Engineering, University of California San Diego, 9500 Gilman Dr., La Jolla, CA 92093, USA

^d University of Lorraine, CRAN, UMR 7039, 2 rue Jean Lamour, 54519 Vandoeuvre-les-Nancy, France

^e CNRS, CRAN, UMR 7039, France

HIGHLIGHTS

- Continuous-time system identification is applied in Lithium-ion battery modeling.
- Continuous-time and discrete-time identification methods are compared in detail.
- The instrumental variable method is employed to further improve the estimation.
- Simulations and experiments validate the advantages of continuous-time methods.

ARTICLE INFO

Article history:

Received 10 May 2016

Received in revised form 1 July 2016

Accepted 2 July 2016

Available online 12 July 2016

Keywords:

Lithium-ion battery

Equivalent circuit model

Battery management system

Continuous-time system identification

Instrumental variable

ABSTRACT

The modeling of Lithium-ion batteries usually utilizes discrete-time system identification methods to estimate parameters of discrete models. However, in real applications, there is a fundamental limitation of the discrete-time methods in dealing with sensitivity when the system is stiff and the storage resolutions are limited. To overcome this problem, this paper adopts direct continuous-time system identification methods to estimate the parameters of equivalent circuit models for Lithium-ion batteries. Compared with discrete-time system identification methods, the continuous-time system identification methods provide more accurate estimates to both fast and slow dynamics in battery systems and are less sensitive to disturbances. A case of a 2nd-order equivalent circuit model is studied which shows that the continuous-time estimates are more robust to high sampling rates, measurement noises and rounding errors. In addition, the estimation by the conventional continuous-time least squares method is further improved in the case of noisy output measurement by introducing the instrumental variable method. Simulation and experiment results validate the analysis and demonstrate the advantages of the continuous-time system identification methods in battery applications.

© 2016 Elsevier Ltd. All rights reserved.

1. Introduction

Lithium-ion batteries have been regarded as a promising candidate for energy storage in electric vehicles due to their acceptable energy and power density compared to other types of energy storage devices [1]. To ensure safe and reliable operation of electric vehicles, the basic conditions of battery packs need to be monitored by the battery management systems (BMS), including voltage, current and temperature. Moreover, some essential states of the batteries also need to be estimated by BMSs, such as

state of charge (SoC), state of health (SoH), and state of power (SoP). Since these states are usually associated with complex electrochemical reactions and cannot be directly measured by physical sensors, researchers need to refer to model-based estimation algorithms.

Among the most commonly applied modeling approaches, the electrochemical model provides high accuracy in estimation since it originates from the first principles of underlying electrochemistry. However, the accurate estimation is achieved at the cost of high complexity in data processing, which requires a significant amount of memory space and computational power to cope with partial differential equations and unknown parameters. This makes this method impractical in real-time applications.

* Corresponding author.

E-mail address: cmi@sdsu.edu (C. Mi).

In contrast, the equivalent circuit model (ECM) is widely accepted in the application level because of its simplicity and ease in online implementation. Equivalent circuit modeling utilizes the system identification techniques to relate the input and output behavior of the battery with circuit elements [2,3]. An n^{th} -order ECM of Lithium-ion batteries is shown in Fig. 1. The n-RC networks can be interpreted as various time domain characteristics of the physical processes and chemical reactions within the battery cell, the series resistance R_0 is the internal resistance of the battery, and the voltage source represents the electrochemical equilibrium potential at different states, also known as open circuit voltage (OCV) [4].

All the aforementioned ECM parameters change as SoC changes, but the parameters can be regarded as constant when SoC variation is small, especially in the carefully designed characterization profiles. The battery characterization determines the best estimates of all the parameters at different SoCs. In general, the OCV is obtained by experiments, and the current and voltage responses in the hybrid pulse power characterization (HPPC) test are used to determine the values of n-RC networks and R_0 at different SoCs [5–8].

Different parameter identification methods can be employed to determine the unknowns. The most common approach uses the so-called indirect approach where the parameters of an equivalent discrete-time model are first estimated from which the continuous-time parameters are then derived in a second step. Numerical searching methods utilize global/local searching algorithms to find the best fit parameters, among which the genetic algorithm (GA) and particle swarm optimization are widely applied [9,10]. The disadvantages of such methods are: (1) the convergence to global optimization is not guaranteed given perturbations, and the result is sensitive to initial condition selection; (2) a constant searching time is not assured, which limits their application in real-time. A more robust method is to use curve fitting tools to fit constant current charging or rest periods of experiment data with exponential functions [11]. The limitation of this method lies in its ignorance of dynamic inputs in tests, thereby resulting into large voltage errors when dynamic inputs are applied. The standard discrete-time least squares (DT LS) method results in the best estimation of battery parameters with both static and dynamic inputs in terms of minimizing the residual. The DT LS method is faster and requires less memory than numerical searching methods. It has been adapted to recursive least squares (RLS) methods and RLS methods with forgetting factor for online estimation [12–15].

As the wide application of the discrete-time model identification in Lithium-ion batteries, researchers have encountered a limitation that the sampling time needs to be chosen with special care. If the sampling time is too large, information on the fast dynamics will be lost, whereas too small a sampling time will result numerical problems, that is, the discrete poles accumulate within a small area close to the boundary of the unit circle [16]. Since the battery system is a typical stiff system with both fast and slow dynamics [17], the selection of sampling time is extremely difficult: rapid

sampling is required to capture the fast dynamics, however, it will lead to large discrepancies in parameter estimation due to the existence of slow dynamics [18,19]. Given limited storage resolution, when the discrete poles are closer to the stability boundary, the discrete system is more prone to numerical precision of the parameters and the location of the discrete poles [20]. It is also concluded by simulation in [21] that the sensitivities to disturbance of the resistance and capacitance values in the RC networks increase quasi-linearly as sampling time decreases, which brings difficulties in accurate system identification.

The direct continuous-time system identification has been studied as opposed to the indirect discrete-time system identification [22,23]. Compared with discrete-time identification methods, the advantages of the continuous-time identification methods are (1) the physical world is continuous and it provides good insight of system properties; (2) the continuous-time identification method avoids discretization that gives rise to undesired high sensitivity issues, and thus can better deal with stiff systems [24]. More detailed differences between continuous-time and discrete-time identification are provided in [18,25].

To the authors' best knowledge, the continuous-time approaches have not been analyzed and compared with discrete-time identification methods in battery applications. The novelty of this paper is (1) the continuous-time system identification methods are utilized to identify system parameters of Lithium-ion batteries; (2) the advantages of continuous-time system identification are demonstrated in detail by analytical analysis, simulation and experiment; (3) The instrumental variable (IV) method is applied to improve the basic continuous-time least squares estimates. In this paper, the continuous-time and discrete-time n^{th} -order ECM are first introduced. Then the system identifiability and sensitivity of the two methods are compared and discussed. Next, a case is studied to identify the parameters of a 2nd-order ECM by continuous-time system identification methods. The continuous-time least squares solution is obtained after a state variable filter (SVF) is applied to pre-process the sampled data, and the estimation is further improved with the IV based estimator for coping with the measurement noise. Simulation and experiment results agree with the analysis and demonstrate the advantages of continuous-time parameter estimation methods in real battery applications.

2. Parameter identification of continuous-time and discrete-time battery models

2.1. Continuous-time battery model

The continuous-time transfer function of the n^{th} -order ECM depicted in Fig. 1 can be written as

$$H(s) = \frac{V_{OCV}(s) - V_{batt}(s)}{I(s)} = \frac{V(s)}{I(s)} \tag{1}$$

$$= \frac{R_1}{R_1 C_1 s + 1} + \frac{R_2}{R_2 C_2 s + 1} + \dots + \frac{R_n}{R_n C_n s + 1} + R_0$$

where $V_{OCV}(s) = \mathcal{L}\{v_{OCV}(t)\}$, $V_{batt}(s) = \mathcal{L}\{v_{batt}(t)\}$, $I(s) = \mathcal{L}\{i(t)\}$, and $\mathcal{L}\{\cdot\}$ is the notation for the Laplace transform.

This function can be rewritten as

$$(s^n + a_1 s^{n-1} + \dots + a_{n-1} s + a_n) V(s) = (b_0 s^n + \dots + b_{n-1} s + b_n) I(s) \tag{2}$$

where all the coefficients are functions of the unknown circuit parameters. Define

$$\theta = [a_1 \ \dots \ a_{n-1} \ a_n \ b_0 \ \dots \ b_{n-1} \ b_n]^T \tag{3}$$

$$= f(R_1, \dots, R_{n-1}, R_n, C_1, \dots, C_{n-1}, C_n, R_0)$$

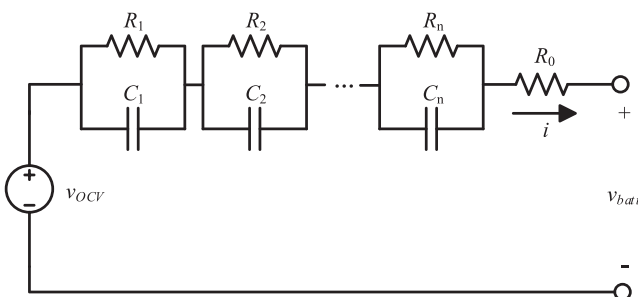


Fig. 1. n^{th} order ECM for Lithium-ion batteries.

where $f: \mathbb{R}^{2n+1} \rightarrow \mathbb{R}^{2n+1}$ maps the circuit parameters to the equation unknowns.

Eq. (2) can be directly written into a regression form as

$$v^{(n)}(t) = \varphi(t)\theta \quad (4)$$

where $v^{(n)}(t)$ denotes the n th time-derivative of $v(t) = v_{OCV}(t) - v_{batt}(t)$, and $\varphi(t)$ is the regression vector given by

$$\varphi(t) = [-v^{(n-1)}(t) \quad \dots \quad -v(t) \quad i^{(n)}(t) \quad \dots \quad i(t)] \quad (5)$$

In practice, the measured terminal voltage of batteries is usually contaminated by noises. Therefore, an equation error $e(t)$ is added to the given regression form. Thus a complete model is given by

$$v^{(n)}(t) = \varphi(t)\theta + e(t) \quad (6)$$

2.2. Discrete-time battery model

To obtain the discrete-time battery model, by using the correct piecewise constant assumption for the current input in HPPC tests, the zero-order hold (ZOH) equivalent of (1) can be derived by (7).

$$H(z) = (1 - z^{-1})\mathcal{Z}\left\{\frac{H(s)}{s}\right\} \quad (7)$$

where $\mathcal{Z}\{\cdot\}$ is the notation for the z-transform.

Thus the continuous-time transfer function (1) yields to

$$H(z) = \frac{V(z)}{I(z)} = \frac{R_1(1 - e^{-\frac{T_s}{R_1 C_1}})}{z - e^{-\frac{T_s}{R_1 C_1}}} + \frac{R_2(1 - e^{-\frac{T_s}{R_2 C_2}})}{z - e^{-\frac{T_s}{R_2 C_2}}} + \dots + \frac{R_n(1 - e^{-\frac{T_s}{R_n C_n}})}{z - e^{-\frac{T_s}{R_n C_n}}} + R_0 \quad (8)$$

and it can be rewritten as

$$(1 + c_1 z^{-1} + \dots + c_n z^{-n})V(z) = (d_0 + d_1 z^{-1} + \dots + d_n z^{-n})I(z) \quad (9)$$

where T_s is the sampling interval, and the coefficients in (9) are functions of the unknown parameters as well as T_s . Define

$$\theta_d = [c_1 \quad \dots \quad c_n \quad d_0 \quad d_1 \quad \dots \quad d_n]^T = g(R_1, \dots, R_{n-1}, R_n, C_1, \dots, C_{n-1}, C_n, R_0, T_s) \quad (10)$$

where $g: \mathbb{R}^{2n+2} \rightarrow \mathbb{R}^{2n+1}$ maps the circuit parameters and T_s to the equation unknowns.

Similar to the continuous-time model, a regression form of (9) with a noise term $\epsilon(k)$ can be written as

$$v(k) = \varphi_d(k)\theta_d + \epsilon(k) \quad (11)$$

where

$$\varphi_d(k) = [-v(k-1) \quad \dots \quad -v(k-n) \quad i(k) \quad i(k-1) \quad \dots \quad i(k-n)] \quad (12)$$

and $v(k)$ denotes the sampled value of $v(t)$ at time-instant t_k .

2.3. System identifiability

The structural identifiability describes the uniqueness of parameters given a dynamic model with noise-free and persistent excitations [26,27]. The battery system is globally identifiable if there is a unique solution $\theta, \theta \in \Theta \subset \mathbb{R}^{2n+1}$, for (6) and (11); the system is locally identifiable if there are a finite number of solutions in Θ ; the system is unidentifiable if there are an infinite number of solutions in Θ .

The identifiability of Randles ECMs are discussed in [28]. The n^{th} -order ECM discussed in this paper has similar structure as that of the Randles models, except for an additional capacitor

connecting in series with the RC networks. Similar derivations hold for the ECM of interest in this paper as well.

Given the continuous system transfer function as (1), if two sets of circuit parameters lead to the same transfer function of an ECM, then

$$\begin{aligned} & \frac{R_1}{R_1 C_1 s + 1} + \dots + \frac{R_n}{R_n C_n s + 1} + R_0 \\ &= \frac{R_1^*}{R_1^* C_1^* s + 1} + \dots + \frac{R_n^*}{R_n^* C_n^* s + 1} + R_0^*, \quad \text{for all } s \end{aligned} \quad (13)$$

A necessary condition for (13) to hold is

$$\left(s + \frac{1}{R_1 C_1}\right) \dots \left(s + \frac{1}{R_n C_n}\right) = \left(s + \frac{1}{R_1^* C_1^*}\right) \dots \left(s + \frac{1}{R_n^* C_n^*}\right), \quad \text{for all } s \quad (14)$$

Since an n degree polynomial is uniquely characterized by its n distinct roots, the assignments of $\left(-\frac{1}{R_1^* C_1^*}, \dots, -\frac{1}{R_n^* C_n^*}\right)$ in (14) need to be the permutations of $\left(-\frac{1}{R_1 C_1}, \dots, -\frac{1}{R_n C_n}\right)$. Assume the order of the distinct roots is strictly defined, i.e. $R_1 C_1 < \dots < R_n C_n$ and $R_1^* C_1^* < \dots < R_n^* C_n^*$. Since the functions of $1/\left(s + \frac{1}{R_i C_i}\right)$ in (14) are linear independent, $R_i C_i = R_i^* C_i^*$ can be obtained and consequently $R_i = R_i^*$ from (13) for $i = 1, 2, \dots, n$. Therefore, all the parameters in the model structure of (1) are uniquely determined. The one-to-one mapping of f in (3) ensures the uniquely determined θ in the reparameterization.

Similar derivation holds for discrete time ECM identifiability. Therefore, the conclusion can be drawn that both continuous-time and discrete-time n^{th} -order ECMs are globally identifiable when the order of the RC networks is strictly defined.

2.4. Sensitivity of discrete-time model poles

The time-constants of an ECM describe essential system properties of the circuit. Physically, they give the time domain characteristics of voltage variations due to different chemical or physical processes upon charge and discharge. The time-constants τ_i in the ECM are calculated by

$$\tau_i = R_i C_i, \quad i = 1, 2, \dots, n \quad (15)$$

Note that the time-constants are closely related to the eigenvalues, or pole locations of the system as

$$\tau_i = \frac{1}{|\lambda_i|}, \quad i = 1, 2, \dots, n \quad (16)$$

where λ_i is the i th eigenvalue of the system.

In order to characterize the fast dynamics of a system, the sampling frequency should be high enough. A rule of thumb [19] is to select a sampling time such that

$$f_s \geq 2 \times \frac{1}{\tau_{\min}} \iff |\lambda_{\max}| T_s \leq \frac{1}{2} \quad (17)$$

where λ_{\max} is the largest eigenvalue, τ_{\min} is its corresponding smallest time-constant in the system, T_s is the sampling time and f_s is the sampling frequency. In practical applications, the sampling frequency f_s is usually set to be higher than the boundary value of $2/\tau_{\min}$ to ensure sufficient sampling.

However, a high sampling rate gives rise to undesirable sensitivity issues as illustrated in Fig. 2. It is well known that the negative real poles in the s -domain map to the interval between the origin and $(1, 0)$ on the real axis of z -domain by (18). As $\lambda_i T_s \rightarrow 0$, the poles in the z -domain approaches $(1, 0)$.

$$z_i = e^{\lambda_i T_s} \quad (18)$$

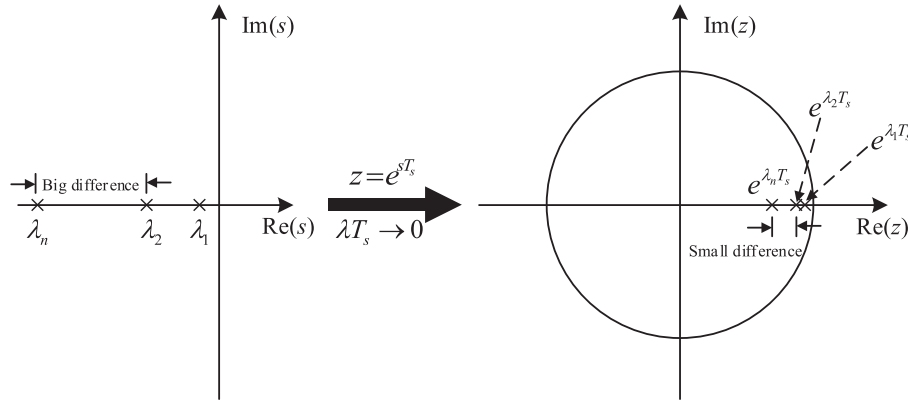


Fig. 2. Discrete pole converges to (1, 0) in z-plane as $\lambda T_s \rightarrow 0$.

Given (16), the sensitivity of the continuous-time model time-constant with respect to z-domain pole location can be derived as (19).

$$S = \left| \frac{z}{\tau} \frac{\partial \tau}{\partial z} \right| = \left| \frac{e^{-\frac{T_s}{\tau}}}{\tau} \frac{\partial \tau}{\partial e^{-\frac{T_s}{\tau}}} \right| = \frac{e^{-\frac{T_s}{\tau}}}{\tau} \frac{\tau^2}{T_s e^{-\frac{T_s}{\tau}}} = \frac{1}{|\lambda| T_s} = \tau f_s \quad (19)$$

The result shows that the sensitivity is the product of sampling frequency and time-constant. Without considering the hardware cost, high sampling frequency is desired so that the discrete-time system is a good approximation of the continuous-time system. However, Eq. (19) implies that faster sampling yields to higher sensitivity of the discrete-time model identification to external disturbances and computation errors.

One can also observe from (19) that the sensitivity is larger for larger time-constants. In a practical on-board battery monitoring system, the sampling frequency can be 100 Hz, and typical time-constant values for 2nd-order ECMs are 30 s and 1000 s [29], thus the sensitivities can be locally as high as 3000 and 100,000 respectively. It indicates that a small variation in z-domain pole estimation leads to a significant change in time-constant estimation. In the extreme condition, as $\lambda T_s \rightarrow 0$, the sensitivity goes to infinity.

It is important to state that such a sensitivity issue stems from the discretization process, and it does not exist in the continuous-time model identification cases.

2.5. Prescaling in fixed-point storage

Most on-board vehicular microprocessors use fixed-point data storage systems. Such representation limits the information that can be stored during calculation due to precision loss and overflow.

In the continuous-time model identification process, given the stiffness of battery systems, the time-constants vary in one or two orders of magnitude. Since the to-be-estimated coefficients are closely related to the multiplication of different pole locations,

these coefficients can be different in several orders of magnitude. If the magnitude of the coefficients is too small, it will lead to big discrepancies in storage, because of the fixed minimum resolution. In order to solve this problem, a parameter prescaling technique is used to maintain the coefficients in the same order of magnitudes, as

$$\tilde{\theta} = U\theta \quad (20)$$

where the prescaling matrix

$$U = \begin{bmatrix} u_1 & 0 & \cdots & 0 \\ 0 & u_2 & \ddots & \vdots \\ \vdots & \ddots & \ddots & 0 \\ 0 & \cdots & 0 & u_{2n+1} \end{bmatrix} \quad (21)$$

and θ is the parameter vector defined in (3).

For instance, if b_n in θ has a magnitude in the order of 10^{-9} , whereas the processor is 16 bits, i.e. the resolution is $2^{-16} = 1.5 \times 10^{-4}$, it is impossible to store b_n in such processor for any further calculation. In this case, u_{2n+1} in U can be set to 10^9 such that $u_{2n+1}b_n$ can be stored properly. Then θ can be retrieved by

$$\theta = U^{-1}\tilde{\theta} \quad (22)$$

In the discrete-time model identification, the dominating poles are close to 1, thus the to-be-estimated coefficients have similar order of magnitudes. Therefore the prescaling is not necessary.

2.6. Summary of the differences between continuous-time and discrete-time model identification

The major differences of continuous-time and discrete-time model identification are listed in Table 1. In summary, the

Table 1
Major differences between discrete-time (DT) and continuous-time (CT) model identification.

	DT	CT
(a)	Uses z-transform	Uses Laplace transform
(b)	Deals with difference equations	Deals with differential equations
(c)	θ_d changes as T_s changes	θ remains unchanged
(d)	DT models are derived from CT, and go back to CT	Remains as CT
(e)	Small T_s or large τ make the system identification sensitive to rounding errors and noises	No undesired sensitivity issues
(f)	Does not have prefiltering	Has inherent prefiltering
(g)	Works easily with fixed-point storage	Requires prescaling in fixed-point storage
(h)	Requires less computation	Requires more computation in filtering

advantages of continuous-time over discrete-time model identification are

- (a) The identified parameters do not change as T_s changes, as shown in (3) and (10), where θ_d is related to T_s .
- (b) High sampling rate to avoid information loss does not lead to undesired high sensitivity issues.
- (c) The continuous-time approach includes inherent filtering, so it is more robust to measurement noises. This is to be discussed in detail in Section 3.
- (d) Additional advantages have been recently discussed and illustrated in [18,23].

The disadvantage of continuous-time model identification are

- (a) The prescaling is required for application in fixed-point storage.
- (b) More computational power is needed to filter the input/output. This is to be discussed in Section 3.

3. Continuous-time identification of battery models

3.1. Conventional least squares based SVF method

The continuous-time model parameter can be obtained from the least squares solution of θ in (6). However, the time-derivatives of the input and output are usually not measured. One traditional approach to handle the time-derivatives measurement problem is to use the state variable filter (SVF) method (see e.g. [16]), which generates filtered (smoothed) versions of the required time-derivatives. A typical SVF is in the form of

$$L_n(s) = \left(\frac{\alpha}{s + \alpha} \right)^n \tag{23}$$

where n is the highest system order, and α determines the cut-off frequency of the SVF. The choice of α is recommended to be slightly higher than the estimated bandwidth of the system [16]. Applying the SVF to (6) yields the linear model as (24).

$$v_{svf}^{(n)}(t) = \varphi_{svf}(t)\theta + e'(t) \tag{24}$$

where $\varphi_{svf}(t) = [-v_{svf}^{(n-1)}(t) \ \dots \ -v_{svf}(t) \ i_{svf}^{(n)}(t) \ \dots \ i_{svf}(t)]$, $v_{svf}^{(n)}(t) = \mathcal{L}^{-1}\{s^n L_n(s)V(s)\}$, $i_{svf}^{(n)}(t) = \mathcal{L}^{-1}\{s^n L_n(s)I(s)\}$, and $\mathcal{L}^{-1}\{\cdot\}$ denotes the inverse Laplace transform.

Based on N sampled measurements of both input and output signals at time instants $t_k, k = 1, \dots, N$, the continuous-time least squares based state variable filter (CT LSSVF) estimator of θ is expressed as

$$\hat{\theta}_{lssvf} = \left[\sum_{k=1}^N \varphi_{svf}^T(t_k) \varphi_{svf}(t_k) \right]^{-1} \sum_{k=1}^N \varphi_{svf}^T(t_k) v_{svf}^{(n)}(t_k) \tag{25}$$

3.2. Improved instrumental variable based SVF method

The least squares solution is unbiased when the equation error is uncorrelated to the regressor, whereas this is usually not true in real applications. In other words, $\hat{\theta}_{lssvf}$ converges to the true parameter θ_0 with the assumption of $E[\varphi_{svf}^T(t_k)e'(t_k)] = 0$, but the least squares regressor $\varphi_{svf}(t)$ contains the measured output voltage, which correlates with $e'(t)$ by (24). In order to make the continuous-time parameter identification consistent for correlated equation errors, the instrumental variable (IV) method is introduced. The main idea of the IV method is to find an instrument $\zeta(t_k)$ whose components are uncorrelated with $e'(t_k)$, i.e. $\frac{1}{N} \sum_{k=1}^N \zeta_{svf}^T(t_k) e'(t_k) = 0$ [30]. The most common IV method utilizes an auxiliary model to generate a noise-free estimate of output, as

$$\zeta_{svf}(t_k) = [-w_{svf}^{(n-1)}(t_k) \ \dots \ -w_{svf}(t_k) \ i_{svf}^{(n)}(t_k) \ \dots \ i_{svf}(t_k)] \tag{26}$$

where $w_{svf}(t_k)$ is the noise-free estimate of voltage calculated by

$$w_{svf}(t_k) = \mathcal{L}^{-1}\{L_n(s)H(s, \hat{\theta}_{lssvf})I(s)\} \tag{27}$$

The continuous-time instrumental variable based state variable filter (CT IVSVF) estimator of θ is given as

$$\hat{\theta}_{ivsvf} = \left[\sum_{k=1}^N \zeta_{svf}^T(t_k) \varphi_{svf}(t_k) \right]^{-1} \sum_{k=1}^N \zeta_{svf}^T(t_k) v_{svf}^{(n)}(t_k) \tag{28}$$

The flow chart for the implementation of n^{th} -order CT IVSVF battery parameter estimator is summarized in Fig. 3.

It can be noticed that there is no further assumption or limitation of the operating conditions of batteries in continuous-time identification, so long as the battery is in its defined normal operating range. In addition, when dealing with stiff systems, the continuous-time identification method does

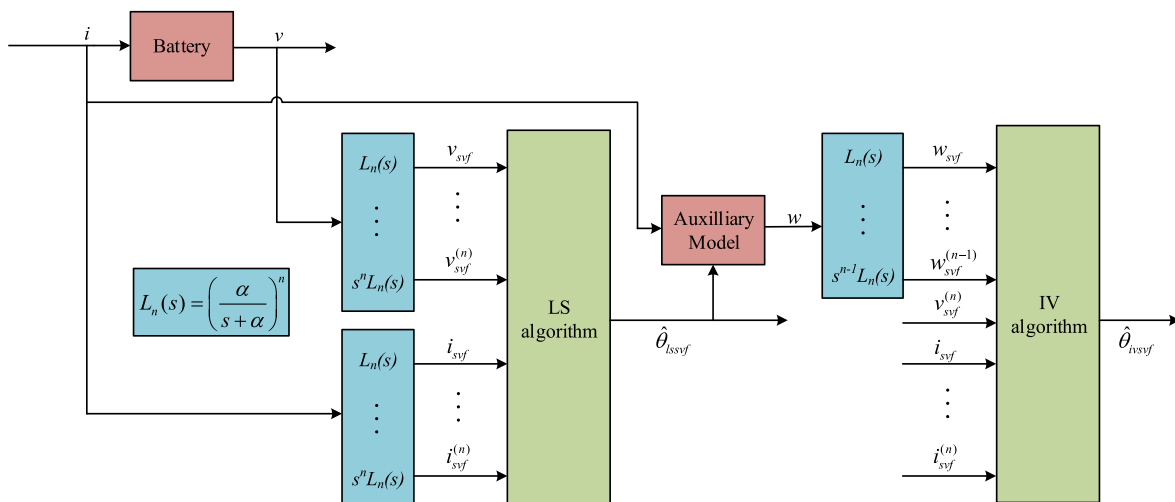


Fig. 3. Implementation flow of CT IVSVF battery parameter estimator.

not require as high storage resolution as discrete-time identification does, because it does not involve numerically dedicate transformation. Therefore, the continuous-time identification methods are expected to have better performance over discrete-time methods, especially when the system is stiff and the storage resolution is limited.

3.3. Model parameterization of the 2nd-order ECM

Based on the analysis in the previous sections, the continuous-time identification methods can be applied to an ECM with any order. In the following sections, the 2nd order ECM is selected because it is the simplest form to present a stiff system. Other than that, [31] concludes that the 2nd order ECM is an optimum choice for implementation of most battery energy and power management strategies.

The continuous-time parameters for the 2nd-order ECM identification are given as

$$\begin{aligned} a_1 &= \frac{1}{R_1 C_1} + \frac{1}{R_2 C_2} \\ a_2 &= \frac{1}{R_1 C_1 R_2 C_2} \\ b_0 &= R_0 \\ b_1 &= R_0 \left(\frac{1}{R_1 C_1} + \frac{1}{R_2 C_2} \right) + \frac{1}{C_1} + \frac{1}{C_2} \\ b_2 &= \frac{R_0 + R_1 + R_2}{R_1 C_1 R_2 C_2} \end{aligned} \quad (29)$$

For comparison purposes, the discrete-time parameters are given as

$$\begin{aligned} c_1 &= - \left(e^{-\frac{T_s}{R_1 C_1}} + e^{-\frac{T_s}{R_2 C_2}} \right) \\ c_2 &= e^{-\left(\frac{T_s}{R_1 C_1} + \frac{T_s}{R_2 C_2} \right)} \\ d_0 &= R_0 \\ d_1 &= -R_0 \left(e^{-\frac{T_s}{R_1 C_1}} + e^{-\frac{T_s}{R_2 C_2}} \right) + R_1 \left(1 - e^{-\frac{T_s}{R_1 C_1}} \right) + R_2 \left(1 - e^{-\frac{T_s}{R_2 C_2}} \right) \\ d_2 &= R_0 e^{-\left(\frac{T_s}{R_1 C_1} + \frac{T_s}{R_2 C_2} \right)} - R_1 e^{-\frac{T_s}{R_2 C_2}} \left(1 - e^{-\frac{T_s}{R_1 C_1}} \right) - R_2 e^{-\frac{T_s}{R_1 C_1}} \left(1 - e^{-\frac{T_s}{R_2 C_2}} \right) \end{aligned} \quad (30)$$

Note that the continuous-time parameters are more complex functions of circuit parameters only, while the discrete parameters are functions of both circuit parameters and T_s , as indicated in (3) and (10).

4. Simulation results

4.1. Simulation setup

Simulations are set up in MATLAB to compare the performance of continuous-time and discrete-time identification methods. In the simulation, the circuit of interest is assumed to have $R_0 = 1 \text{ m}\Omega$, $R_1 = 0.3 \text{ m}\Omega$, $R_2 = 0.6 \text{ m}\Omega$, $\tau_1 = 30 \text{ s}$ and $\tau_2 = 1000 \text{ s}$, and the capacity of the battery is 40 Ah. It needs to be noticed that the simulated system is a typical stiff system, because it includes a fast and a slow time-constants.

The input excitation is shown in Fig. 6c. It consists of five pairs of discharge and charge pulses, each lasting for 20 s. The amplitude of the pulse pairs are 0.5C, 1.0C, 1.5C, 2.0C and 2.5C, respectively, where C is a measure of current at which a battery is discharged to its nominal capacity. The rest periods after each discharge pulses

are 40 s, and the rest periods after each charge pulses are 60 s. After the five pair of pulses, a 0.5C 2% SoC discharge is applied, followed by a 1-hr rest.

Various sampling intervals are used in the simulation, which are set to be 1 s, 0.1 s, and 0.01 s, respectively. White Gaussian noises with different signal to noise ratios (SNR) are added to the voltage output in the simulation to emulate the measurement noise of the system, such that

$$v(k) = v_{det}(k) + n(k) \quad (31)$$

where v_{det} is the deterministic (or noise-free) voltage signal, $n(k)$ is the measurement noise added to the noise-free voltage signal, and $v(k)$ is the noisy voltage measurement.

The SNR is defined as

$$\text{SNR}_{\text{dB}} = 10 \log_{10} \frac{\sigma_{v_{det}}^2}{\sigma_n^2} \quad (32)$$

where $\sigma_{v_{det}}^2$ is the variance of v_{det} and σ_n^2 is the variance of the added noises. The standard deviation of noises are chosen to be 0.01 mV, 1 mV and 10 mV respectively. Therefore the corresponding SNR values are 62 dB, 22 dB and 2 dB, respectively.

The SVF cut-off frequency is 0.01 rad/s. Unless otherwise specified, the intermediate data storage for all the simulation is 16 bits, and the prescaling technique introduced in Section 2.5 is applied to all simulation.

Monte Carlo simulations are used to evaluate the performance of the model identification methods, such that 100 different noise realizations are generated for each of the sampling intervals and noise levels. The Bode plots of the identified systems are presented for different methods in various conditions. Except DT LS, CT LSSVF and CT IVSVF methods, it is also interesting to see the performance of DT LS method with the same pre-filtering as in the continuous-time methods, as suggested by [12]. The Bode plots of estimated models based on discrete-time methods are presented in Fig. 4, and those based on continuous-time methods are presented in Fig. 5.

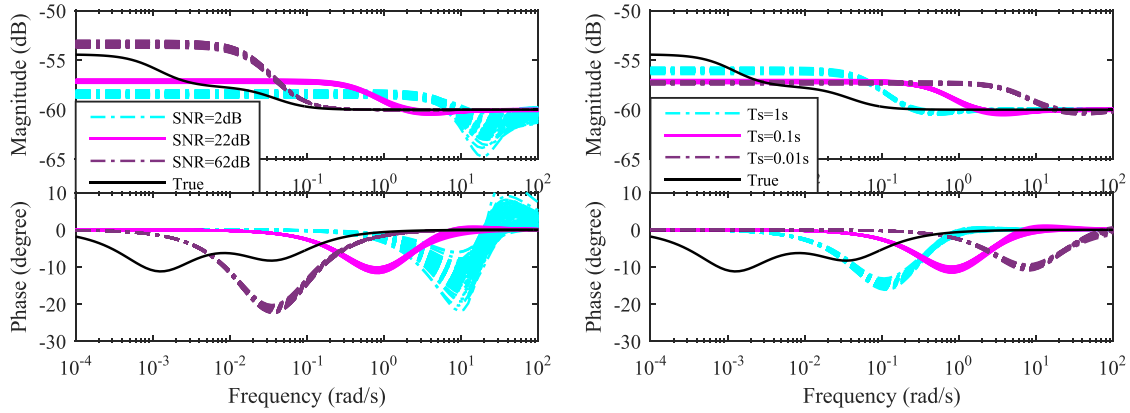
4.2. Discussion of simulation results

Fig. 4a and b give the Bode plots for the CT models identified by the indirect DT LS-based method. The identified models are clearly biased at the low frequency ends. As the noise level or sampling rate increases, the identified systems are more biased.

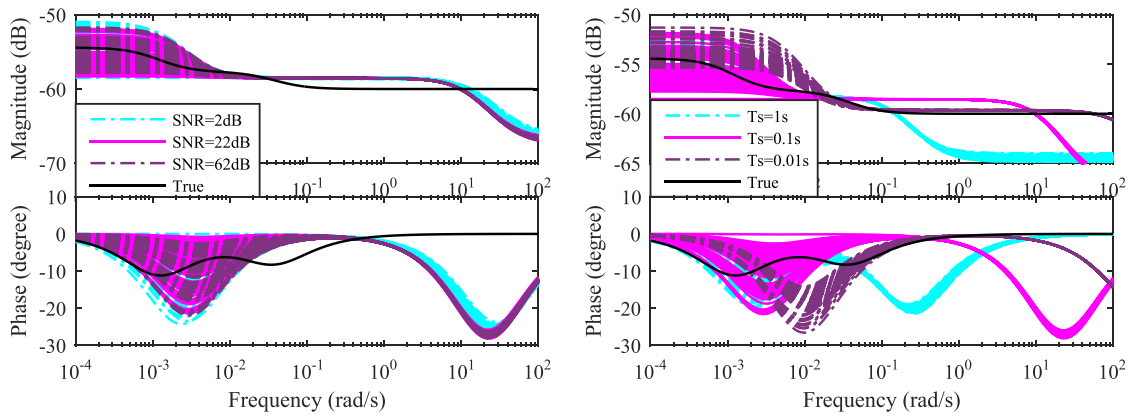
The Bode plots for the systems identified by the DT LS methods with both input and output filtering are given in Fig. 4c and d. The filter applied is the same as $L_2(s)$ with same cut-off frequency as SVF. It is hard to conclude solely from the two plots whether the pre-filtering improves the system identification, but at least the pre-filtering does not provide the desired system identification. Later simulation with 64 bit storage resolution in Fig. 4e and f demonstrates the effectiveness of the pre-filtering in high storage resolutions. The difference in the identification performance indicates that the pre-filtering is largely influenced by the rounding errors in discrete-time identification.

Fig. 5a and b present the identification results of CT LSSVF method in various conditions. The performance of system identification is remarkably improved, which is due to the application of data pre-filtering and avoidance of discretization.

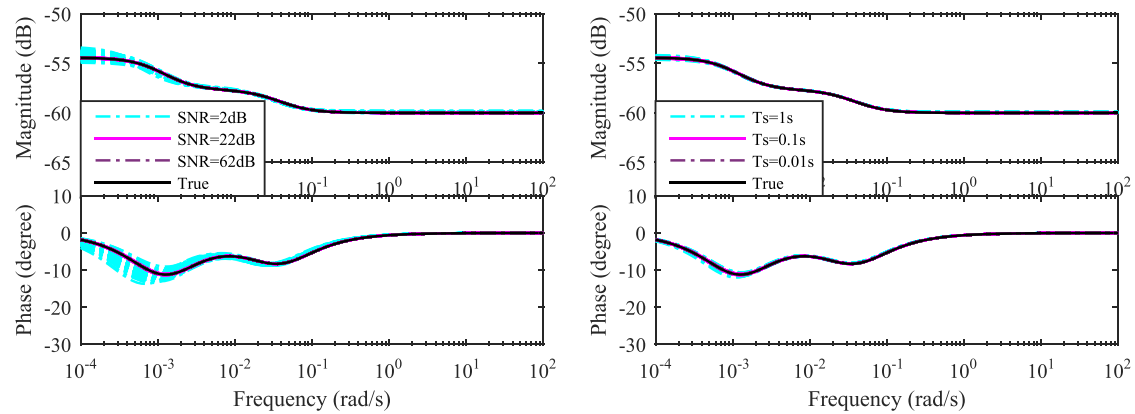
At last, Fig. 5c and d show that CT IVSVF identification has accurate identifications in all situations, where the Bode plots of the identified systems overlap that of the true system with a high fidelity except when the SNR is equal to 2 dB when a bias can be observed in the low-frequency part of the response.



(a) DT LS method for different SNR ($T_s=0.1$ s, 16 bits). (b) DT LS method for different T_s (SNR=22dB, 16 bits).



(c) DT LS method with pre-filtering for different SNR ($T_s=0.1$ s, 16 bits). (d) DT LS method with pre-filtering for different T_s (SNR=22dB, 16 bits).



(e) DT LS method with pre-filtering for different SNR ($T_s=0.1$ s, 64 bits). (f) DT LS method with pre-filtering for different T_s (SNR=22dB, 64 bits).

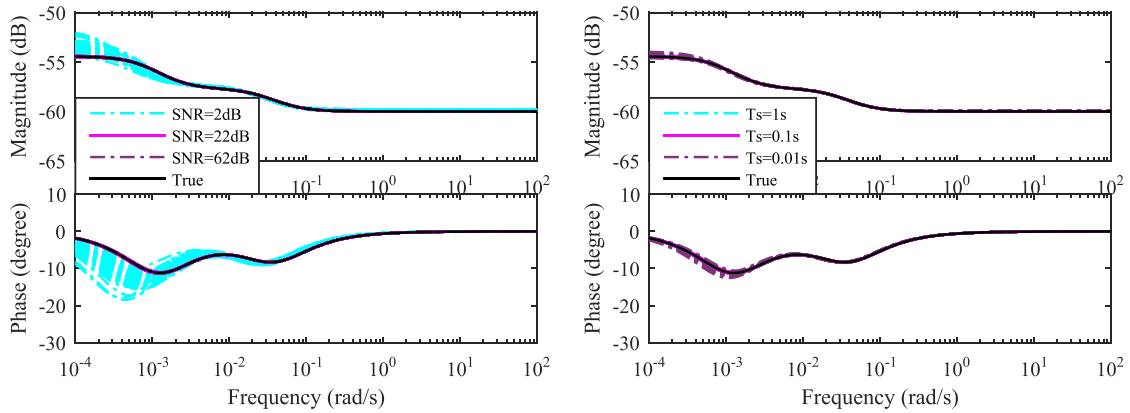
Fig. 4. Monte Carlo simulation with different SNR and T_s . Bode plots of CT models from indirect DT methods.

In summary, most of the indirect discrete-time identification methods lead to large discrepancies in system identification, especially in the presence of noises and small sampling intervals; the simple CT LSSVF estimates are clearly less biased due to SVF pre-filtering and low sensitivity to rounding errors, and the CT IVSVF estimates are both accurate and robust in all situation.

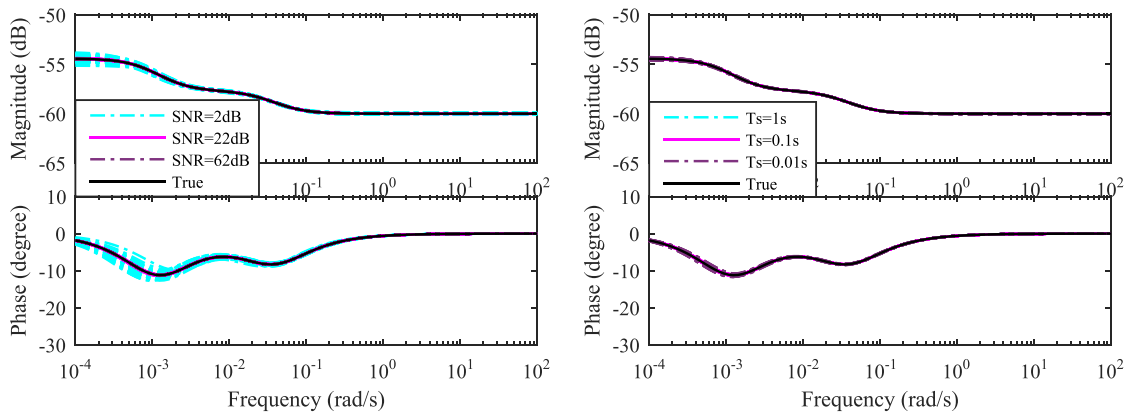
5. Experimental results

5.1. Battery tests

In order to identify the parameters of a Lithium-ion polymer cell, battery characterization experiments are conducted at room



(a) CT LSSVF method for different SNR ($T_s=0.1$ s, 16 bits). (b) CT LSSVF method for different T_s (SNR=22dB, 16 bits).



(c) CT IVSVF method for different SNR ($T_s=0.1$ s, 16 bits). (d) CT IVSVF method for different T_s (SNR=22dB, 16 bits).

Fig. 5. Monte Carlo simulation with different SNR and T_s . Bode plots of CT models from direct CT methods.

Table 2
Specification of battery under test.

Material	Lithium-ion polymer
Charge/discharge capacity	40.83/40.61 Ah
Nominal voltage	3.7 V
Maximum charge voltage	4.2 V
Minimum discharge voltage	2.7 V

temperature (22–25°C). The specification of the battery under tests is given in Table 2. The procedure of the characterization tests is shown in Fig. 6a. The sampling rate in all the experiments is 1 Hz.

The capacity test consists of three charge/discharge cycles. In each cycle, the battery is charged with a constant current of 0.5C until the terminal voltage reaches the maximum charge voltage. Then the voltage is kept at the maximum charge voltage until the charge current is below 1/20C. After that, the battery is discharged at 0.5C until the minimum discharge voltage is reached.

A 1 hr rest is applied after each charge/discharge operation. The charge/discharge capacity are calculated as the average value of the three cycles.

The charge/discharge OCV-SoC curves are obtained at 10% SoC step with 0.5C charge/discharge rate and 5 hr rest, as shown in Fig. 6b. It can be observed that the charge OCV curve is higher than the discharge curve due to the hysteresis effect. The maximum difference between charge/discharge curves is 22.6 mV. The average value of charge/discharge OCV curves is used in the model calculation for simplicity.

The HPPC test profile is the same as mentioned in Section 4. The HPPC test is repeated between 10% and 90% SoC with 2% SoC step. The current input and voltage output of the HPPC pulses at SoC = 50% are shown in Fig. 6d.

Finally, Urban Dynamometer Driving Schedule (UDDS) cycles with 10 min rest periods are applied consecutively to the battery cell to validate the identified model. The initial SoC for UDDS test is 90%, and the test is terminated after the first cycle when SoC drops below 20%. The current profile of UDDS is scaled such that the maximum discharge current is 100 A.

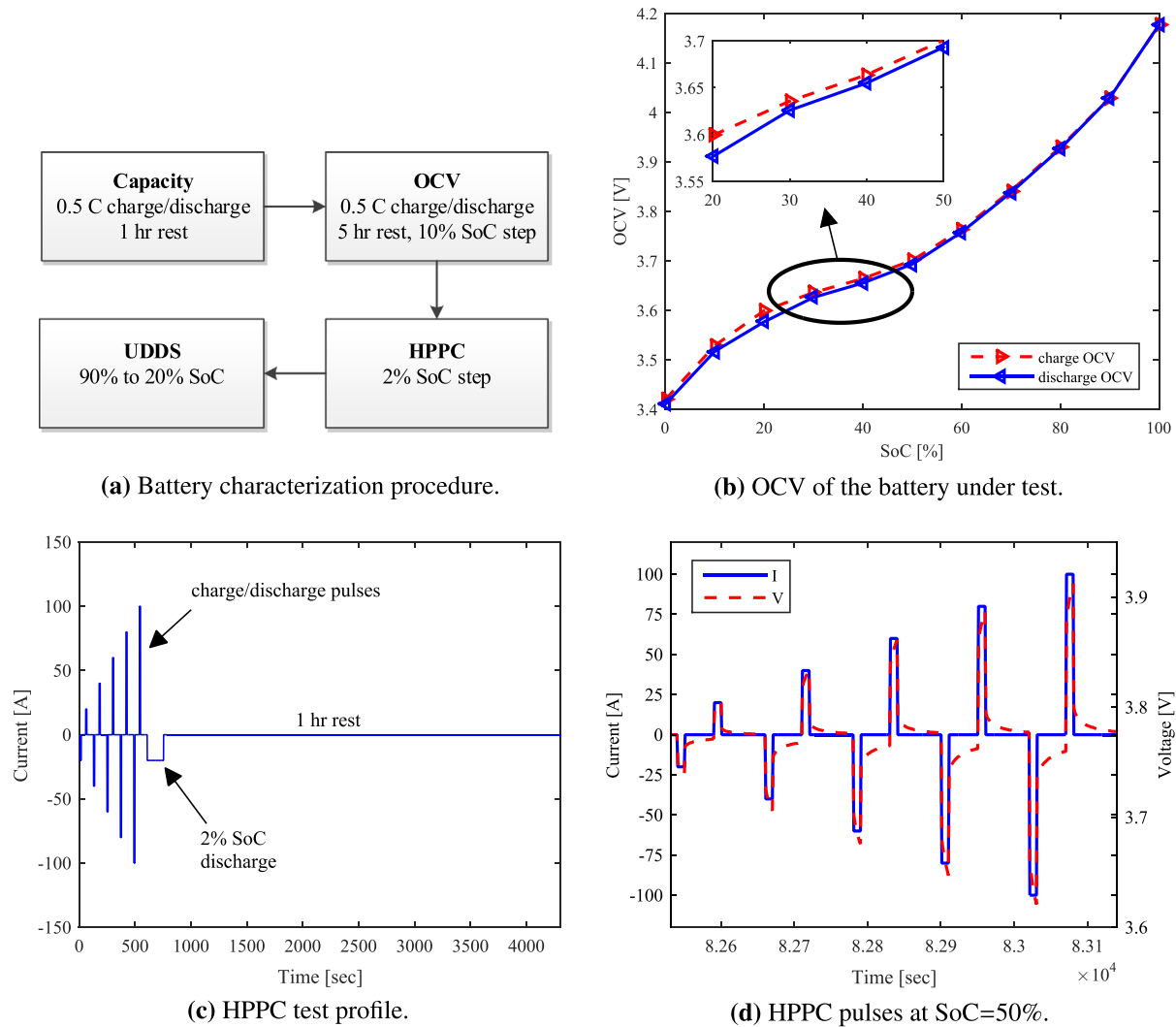


Fig. 6. Battery characterization and validation experiments.

5.2. Discussion of experimental results

In order to demonstrate the advantages of continuous-time system identification, the performances of CT LSSVF and CT IVSVF estimators are compared with DT LS method and DT LS with pre-filtering. The cut-off frequency for both of the filters are 0.025 rad/s and the storage resolution is 16 bits.

The voltage outputs of the simulated models and experiments in UDDS are plotted in Fig. 7a, and the zoomed-in range between 5900 s and 7400 s are shown in Fig. 7b. The results show that

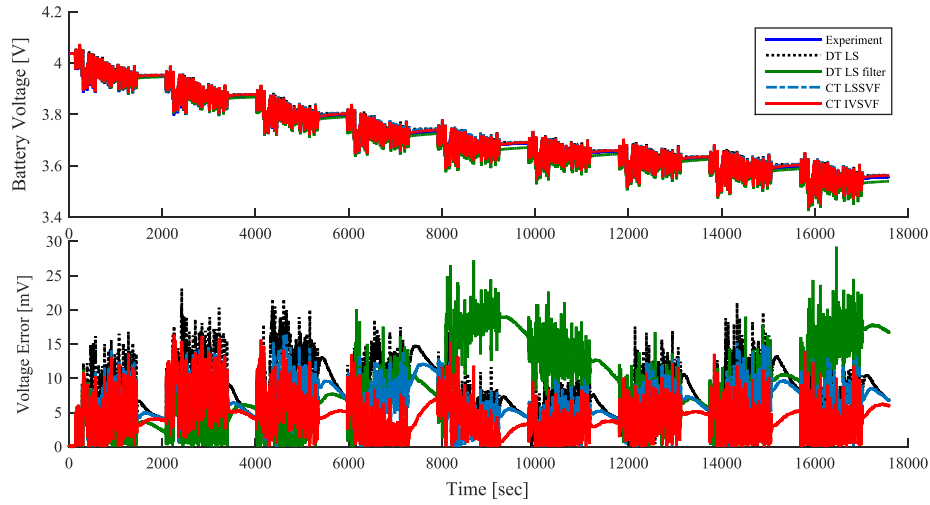
- The indirect discrete-time methods have the larger overall error.
- The DT LS method with pre-filtering has similar noise levels to the CT LSSVF method in some of the cycles, however, the systems identified are clearly biased in the 5th, 6th and 9th cycle. The defect in robustness is mainly caused by its high sensitivity to unmodeled dynamics and colored noises in the experiment.
- The two direct continuous-time identification methods have better performance over other methods. Furthermore, CT

IVSVF estimator gives better estimation because the newly introduced instrumental variable is less correlated to equation error.

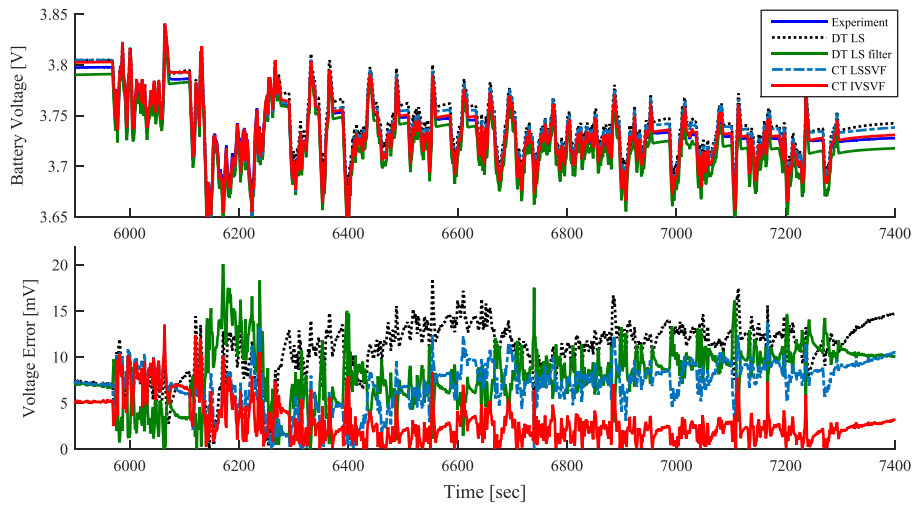
Based on the findings in simulation results, the DT LS method tends to estimate the poles of the system to be larger, then the corresponding time-constants are smaller. This can be observed in Fig. 8 as well, where the time-constant estimates of DT LS are the smallest among all the methods.

It needs to be noticed that DT LS presents acceptable results in experiments because the UDDS cycle mainly consists of high frequency contents, where it gives reasonable identification in the simulation as well. However, it has large bias in larger time-constant estimates, which will lead to larger discrepancies when the input is constant. This can be visualized by its larger discrepancies at beginning of rest periods between UDDS cycles.

The mean absolute error (MAE) and root mean squares error (RMSE) of the aforementioned estimators within the whole experimental period are listed as in Table 3. It validates that the continuous-time identification methods have better overall performance and CT IVSVF method gives voltage estimations with the smallest error.

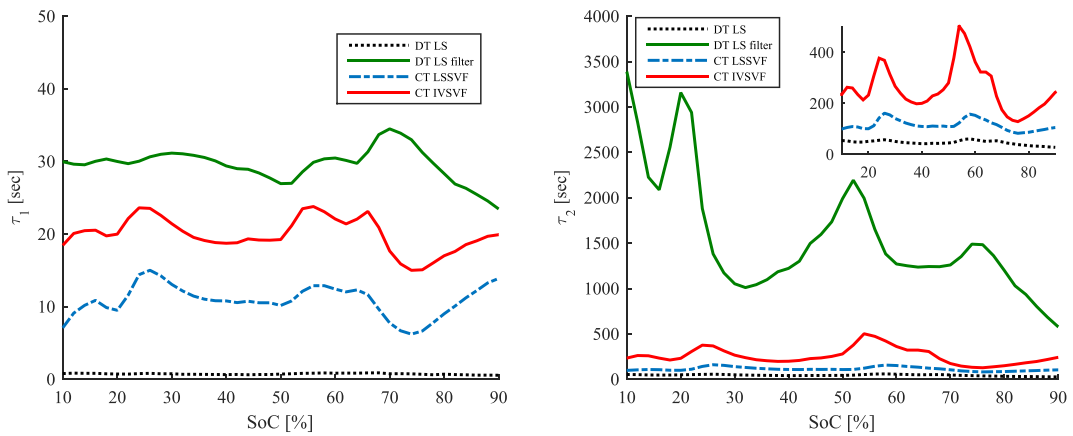


(a) Voltage values and errors across all UDSS tests.



(b) Detailed voltage values and errors for 5,900 s and 7,400 s.

Fig. 7. Discrepancies of different identification methods.



(a) τ_1 estimates.

(b) τ_2 estimates.

Fig. 8. Time-constant estimates from experimental data with different methods.

Table 3
MAE and RMSE of model voltage estimation in whole UDDS validation.

	DT LS	DT LS filter	CT LSSVF	CT IVSVF
MAE [mV]	8.59	8.71	6.34	4.27
RMSE [mV]	9.35	10.36	6.96	4.95

6. Conclusion

This paper has presented the advantages of continuous-time system identification methods in battery ECM parameter estimation. The combination of fast dynamics induced by charge transfer and slow dynamics from diffusion causes the dynamics of a battery to exhibit stiff system behavior. Continuous-time identification reduces the sensitivity of the model parametrization in case of a stiff dynamic system, leading to improvements on battery parameter estimation in simulation and experiment results, especially when battery dynamic parameters are stored in fixed precision.

The general modeling of both continuous-time and discrete-time n^{th} -order ECM is first discussed. Then it is shown that the n^{th} -order ECM is identifiable if the order of the time-constants is strictly defined. The comparison between continuous-time and discrete-time methods indicates that discrete-time identification methods are less robust due to undesired sensitivity issues in transformation of discrete domain parameters. In continuous-time parameter identification, SVF is used to smoothen the time-derivative terms. After that, the IV method is applied to further increase the estimation accuracy by reducing the correlation between equation error and regressor.

Simulation results show that the continuous-time identification methods demonstrate higher accuracy in stiff system estimations given different sampling intervals and noise levels, because of the inherent SVF pre-filtering and the avoidance of pole discretization. Characterization experiments are conducted and different identification methods are used to identify the battery parameters, including DT LS, DT LS with pre-filtering, CT LSSVF and CT IVSVF. The results indicate that the continuous-time identification methods results in the smallest mean absolute error and root mean square error. Among all, the best output voltage prediction is obtained by CT IVSVF method.

This research bridges the gap between battery parameter estimation algorithm development and real applications, where the system is stiff and the storage resolutions are limited. It is important to note that the offline continuous-time parameter estimation can be easily adapted online. With a more accurate battery model, the estimation of other battery states can be improved accordingly, such as SoC, SoH and SoP. The future work includes the implementation of the improved recursive continuous-time system identification methods to battery online state estimation.

Acknowledgements

The authors would like to acknowledge the funding support from Nanjing Golden Dragon Bus Co., Ltd., and the U.S. Department of Energy under the Graduate Automotive Technology Education Center program.

References

[1] Lu L, Han X, Li J, Hua J, Ouyang M. A review on the key issues for lithium-ion battery management in electric vehicles. *J Power Sources* 2013;226:272–88.

[2] Hu X, Li S, Peng H. A comparative study of equivalent circuit models for li-ion batteries. *J Power Sources* 2012;198:359–67.

[3] Sun F, Xiong R. A novel dual-scale cell state-of-charge estimation approach for series-connected battery pack used in electric vehicles. *J Power Sources* 2015;274:582–94.

[4] Monem MA, Trad K, Omar N, Hegazy O, Mantels B, Mulder G, Van den Bossche P, Van Mierlo J. Lithium-ion batteries: evaluation study of different charging methodologies based on aging process. *Appl Energy* 2015;152:143–55.

[5] Xiong R, Sun F, Chen Z, He H. A data-driven multi-scale extended Kalman filtering based parameter and state estimation approach of lithium-ion Olymer battery in electric vehicles. *Appl Energy* 2014;113:463–76.

[6] Han X, Ouyang M, Lu L, Li J. A comparative study of commercial lithium ion battery cycle life in electric vehicle: capacity loss estimation. *J Power Sources* 2014;268:658–69.

[7] Chen Z, Xia B, Mi CC, Xiong R. Loss-minimization-based charging strategy for lithium-ion battery. *IEEE Trans Indust Appl* 2015;51(5):4121–9.

[8] Sun F, Xiong R, He H. A systematic state-of-charge estimation framework for multi-cell battery pack in electric vehicles using bias correction technique. *Appl Energy* 2016;162:1399–409.

[9] Seaman A, Dao T-S, McPhee J. A survey of mathematics-based equivalent-circuit and electrochemical battery models for hybrid and electric vehicle simulation. *J Power Sources* 2014;256:410–23.

[10] Fleischer C, Waag W, Heyn H-M, Sauer DU. On-line adaptive battery impedance parameter and state estimation considering physical principles in reduced order equivalent circuit battery models: Part 1. Requirements, critical review of methods and modeling. *J Power Sources* 2014;260:276–91.

[11] Chen M, Rincon-Mora GA. Accurate electrical battery model capable of predicting runtime and I–V performance. *IEEE Trans Energy Convers* 2006;21(2):504–11.

[12] Fridholm B, Wik T, Nilsson M. Robust recursive impedance estimation for automotive lithium-ion batteries. *J Power Sources* 2016;304:33–41.

[13] Tang X, Mao X, Lin J, Koch B. Li-ion battery parameter estimation for state of charge. In: American control conference (ACC), San Francisco; 2011. p. 941–6.

[14] Kim T, Wang Y, Fang H, Sahinoglu Z, Wada T, Hara S, et al. Model-based condition monitoring for lithium-ion batteries. *J Power Sources* 2015;295:16–27.

[15] Xia B, Chen C, Tian Y, Wang M, Sun W, Xu Z. State of charge estimation of lithium-ion batteries based on an improved parameter identification method. *Energy* 2015;90:1426–34.

[16] Garnier H, Mensler M, Richard A. Continuous-time model identification from sampled data: implementation issues and performance evaluation. *Int J Control* 2003;76(13):1337–57.

[17] Remmlinger J, Buchholz M, Meiler M, Bernreuter P, Dietmayer K. State-of-health monitoring of lithium-ion batteries in electric vehicles by on-board internal resistance estimation. *J Power Sources* 2011;196(12):5357–63.

[18] Garnier H, Young PC. The advantages of directly identifying continuous-time transfer function models in practical applications. *Int J Control* 2014;87(7):1319–38.

[19] Rao GP, Sinha NK. Continuous-time models and approaches. In: Identification of continuous-time systems. Springer; 1991. p. 1–15.

[20] Wu H, Yuan S, Zhang X, Yin C, Ma X. Model parameter estimation approach based on incremental analysis for lithium-ion batteries without using open circuit voltage. *J Power Sources* 2015;287:108–18.

[21] Yuan S, Wu H, Ma X, Yin C. Stability analysis for li-ion battery model parameters and state of charge estimation by measurement uncertainty consideration. *Energies* 2015;8(8):7729–51.

[22] Garnier H, Wang L, editors. Identification of continuous-time models from sampled data. London: Springer; 2008.

[23] Garnier H. Direct continuous-time approaches to system identification. Overview and benefits for practical applications. *Eur J Control* 2015;24:50–62.

[24] Garnier H, Bitmead RR, de Callafon R. Direct continuous-time model identification of high-powered light-emitting diodes from rapidly sampled thermal step response data. In: 19th Triennial IFAC world congress on automatic control, Cape Town, South Africa.

[25] Rao G, Unbehauen H. Identification of continuous-time systems. IEE proceedings- control theory and applications, vol. 153.

[26] Godfrey K, DiStefano III J. Identifiability of model parameters. Identifiability of parametric models 1987:1–20.

[27] Bellman R, Åström KJ. On structural identifiability. *Mathematical biosciences* 1970;7(3):329–39.

[28] Alavi SM, Mahdi A, Payne SJ, Howey DA. Structural identifiability of battery equivalent circuit models. Available from: arXiv:1505.00153.

[29] Jiang J, Liu Q, Zhang C, Zhang W. Evaluation of acceptable charging current of power li-ion batteries based on polarization characteristics. *IEEE Trans Indust Electron* 2014;61(12):6844–51.

[30] Young PC. Recursive estimation and time-series analysis: an introduction for the student and practitioner. second edition. Berlin: Springer-Verlag; 2011.

[31] Nejad S, Gladwin D, Stone D. A systematic review of lumped-parameter equivalent circuit models for real-time estimation of lithium-ion battery states. *J Power Sources* 2016;316:183–96.